STUDY OF SWIRL ATOMIZERS FOR LIQUID PROPELLANT ROCKET ENGINES USING AN OPEN SOURCE CFD CODE

Brunno Barreto Vasques, brunno04017@yahoo.com
Wladimyr Mattos C. Dourado, wladimyr@iae.br
Instituto de Aeronáutica e Espaço, Praça Marechal Eduardo Gomes, 50, 12228-904 São José dos Campos, Brasil

Marcio Teixeira de Mendonça, marcio@ita.br
Instituto Tecnológico de Aeronáutica, Praça Marechal Eduardo Gomes, 50, 12228-900 São José dos Campos, Brasil

Abstract. *This work attempts to establish the vision for Computational Fluid Dynamics as a rocket injector design tool. Simulations of a 5-kN thrust liquid rocket engine swirl atomizer, under cold flow conditions, using an open source CFD code is the immediate goal of this research. Swirl atomizers are considered a low cost and reliable type of atomizer for propellant injection due to its good atomization characteristics and inherently simple geometry, being the heart of most Russian liquid rocket combustion chambers. The governing equations are solved based on the laminar volume of fluid (VOF) interface capturing method. The oxidizer and fuel injector elements were analyzed for discharge coefficient, spray-cone angle, liquid film thickness as well as other design related parameters. Results from cold flow experiments and particle image velocimetry (PIV) are compared to the predictions of the swirl models and the numerical results. The laminar VOF model was able to predict the spray angle with reasonable confidence, however, a deviation of 25 % was observed in the mass flow rate and discharge coefficient. Although the laminar VOF model has proven inadequate, it constitutes a good starting point in the procedure needed to assess swirl injector performance.*

Keywords: *Swirl atomizers, liquid propellant rocket engines, computational fluid dynamics.*

1. INTRODUCTION

Swirl injectors have been employed in a wide variety of areas such as crop dusting, fire protection, industrial furnaces, gas turbines, diesel engines and, of course, rocket engines. Swirl atomizers are considered a low cost and reliable type of atomizer for propellant injection due to its good atomization characteristics and inherently simple geometry. Since swirl atomizers provide throttling capability (Bazarov, 1985) and high-thrust per element, they have been intensely applied in aerospace propulsion systems for over the past 60 years.

From the standpoint of operational requirements, it is highly desirable to conceive atomizers capable of producing sprays with predetermined droplet size distribution at the appropriate combustor location, thus providing an uniform heat release from the combustion process.

An important feature of swirl injectors is their intense dynamic coupling with upstream and downstream perturbations, as well as instabilities arising from the atomizer internal flow. In rocket propulsion applications, dynamic characteristics are important to predict injector performance and establish a better understanding of combustion instability phenomena related to the engine dynamic response.

The workings of a hollow-cone swirl atomizer can be explained with reference to Fig.1. It is composed mainly of tangential channels, a swirl chamber and an exit nozzle. The liquid enters the swirl chamber tangentially under the supply pressure, where due to geometry, it is caused to rotate about the center axis creating a free vortex inside the chamber. The swirl velocity obeys a constant-divided-by-radius velocity profile, which is dependent on entry conditions. This relationship between swirl velocity and radius means that the swirl velocity is highest at small radii, so much so that according to the pressure-velocity relationship of Bernoulli, the pressure there reduces to match that of the ambient medium into which the liquid is subsequently ejected. This allows the medium to enter along the axis of the atomizer to form a hollow “air" core. Thus if the liquid is discharged to the atmosphere, the radius of the air core occurs at that position where, due to the magnitude of the dynamic (velocity) head, the static pressure has become zero gauge.

The dynamic head is constant all along the surface of the air core as the pressure there is constant at a given ambient medium pressure. However, due to continuity, the axial velocity is greater in the smaller-diameter outlet than in the swirl chamber. This means that the swirl velocity on the air core in the outlet must be smaller than that on the air core in the swirl chamber. This can only be so, as the swirl is constant for any radius throughout the axial length of the atomizer, and it decreases with increasing radius, then the radius at which the static pressure equals that of the ambient medium must be greater than in the swirl chamber in order for the net velocity head be equal to the constant total pressure, given by the Bernoulli equation.

Over this description of “ideal fluid" within the swirl atomizer, there are real fluid effects. These include the effects of viscosity on the wall boundaries of the flow domain and friction losses in the inlet channels, which will act to retard the flow of the liquid and effectively alter the perceived atomizer dimensions from the ideal fluid scenario. In particular, in reducing the diameter of the outlet orifice. Also, turbulence effects will alter the flow regime from the ideal case. This

poses significant difficulties to the solution of atomizer flow. A handful of analytical models, experimental and numerical methods have been employed in an attempt to describe the flow behavior inside swirl injectors.

The most notable efforts in the West to model the flow inside swirl atomizers were published by G. Taylor (1948) and again a few years later by Giffen and Muraszew (1953). In the Soviet Union, the works of V. A. Glushko in 1932 and G. N. Abramovich (1946) in the late 40's set a standard methodology for swirl injector design. Recently, J. J. Chinn (2009) revisited swirl injector theory with reference to the *principle of maximum flow* to elucidate and compare the analyses of Giffen and Muraszew (1953), G. N. Abramovich (1944) and G. Taylor (1948). This study concluded that the mentioned authors have all conceived of essentially the same inviscid formulation for pressure swirl atomizer internal flow.

The effect of swirler geometric parameters on spray characteristics has been experimentally investigated by Kim et al. (2007) and more recently, by Chu et al. (2008). Although not all geometric parameters can be investigated, these experimental studies contribute to validate the usefulness of most analytical models.

Attempts were also made numerically to explore the underlying mechanisms of fluid injection and combustion. Recently, an interesting investigation was conducted by Hinckel et al. (2008). The purpose of this work was to determine the accuracy of the original well-known Abramovich solution (Vasiliev et al., 1993) and other non-ideal flow solutions. The numerical solution was relied upon a commercial CFD package and the standard $\kappa - \epsilon$ turbulence model. The CFD model agreed qualitatively well with the available experimental results, and discrepancies were attributed to the large mass flows employed in the experiments. More recently, Park and Heister (2010) simulated the atomization processes in a pressure-swirl atomizer via axisymmetric boundary element method. The implementation provided a first-principles capability to simulate drop size distributions for low viscosity fluids.

2. THE ABRAMOVICH ANALYTICAL MODEL

Modeling the inviscid flow physics of a swirl injector represents a great challenge to swirl injector design. The fluid enters the swirl chamber off axis at the velocity W_{in}, forms a circumferential swirling flow, exhausts at the axial velocity W_{an} through the nozzle and finally establish a near-conic sheet in the mixture-formation zone. Ideally, the liquid sheet has the shape of a hyperboloid of revolution. The spray angle is determined by the ratio of tangential and axial velocities at the nozzle exit, as given by Equation (1):

$$\alpha = \arctan\left(\frac{W_{un}}{W_{an}}\right) \tag{1}$$

where α is the spray cone half angle and W_{un} and W_{an} are the tangential and axial components of velocity at nozzle exit, respectively.

Several models exist to describe the relationship between the atomizer geometry and the flow characteristics of the swirl injector. Each of these models made the following assumptions:

- Incompressible flow;
- Inviscid flow;
- Gravity and surface effects are negligible;
- Angular momentum is constant.

The second assumption translates into irrotational flow. In other words, $\nabla \times \vec{W} = \vec{0}$. This condition is used to describe the conservation of angular momentum inside the atomizer:

$$rW_u = constant \tag{2}$$

or, between the inlet channels and other arbitrary point in the injector,

$$W_{in}R_{in} = W_u r \tag{3}$$

The liquid potential energy in the form of pressure drop across the injector is fully converted to kinetic energy. Hence, the total liquid flow velocity is:

$$W = \sqrt{\frac{2}{\rho}\Delta p_{inj}} = \sqrt{W_u^2 + W_a^2 + W_r^2} \tag{4}$$

where Δp_{inj} is the pressure drop across the injector.

The radial component of velocity, W_r is assumed negligible, hence

$$W = \sqrt{W_{uk}^2 + W_{ak}^2} = \sqrt{W_{un}^2 + W_{an}^2} = W_{uo} \tag{5}$$

The subscripts o, k and n denote the conditions at the injector head end, vortex chamber and nozzle, respectively. At the injector head end, $W_a = 0$. The circumferential component of the liquid velocity W_{uo} is maximum and the radius of liquid-vortex surface, on the contrary, is minimum. In the vortex chamber, the axial velocity W_{ak} is positive and the circumferential velocity is W_{uk} is smaller than W_{uo}, giving $r_{gk} > r_{go}$. In the nozzle, the smaller liquid passage area leads to an increase of the axial velocity W_{an} and a decrease of W_{un}, giving $r_{gn} > r_{gk}$. Finally, at the nozzle exit, the centrifugal force arising from the swirling motion acts as a velocity head, leading to an additional increase of the axial velocity and subsequently an increase of the liquid-surface radius.

Since a gas core must be present, otherwise, from Equation (2), the angular velocity would be *infinite*, the liquid will not fully occupy the entire injector. Thus, a *coefficient of useful cross section*, φ, that relates the area filled by the liquid to the nozzle area, can be defined:

$$\varphi = \frac{\pi(r_n^2 - r_{gn}^2)}{\pi r_n^2} = 1 - \frac{r_{gn}^2}{r_n^2} \tag{6}$$

Various geometric parameters can be correlated to form a non-dimensional *geometrical characteristic parameter*, K, defined as:

$$K = \frac{R_{in} r_n}{n r_{in}^2} \tag{7}$$

where R_{in} is radial location of the tangential passages, r_n is the nozzle radius, n is the number of tangential channels and r_{in} is the radius of the tangential inlet passage. The *contraction ratio*, C, relates the radial location of inlet channels to the nozzle radius:

$$C = \frac{R_{in}}{r_n} \tag{8}$$

The mass flow rate through the atomizer can be obtained in terms of the non-dimensional injector parameters:

$$\dot{m}_{inj} = \frac{\pi r_n^2}{\sqrt{\frac{1}{\varphi^2} + \frac{K^2}{1-\varphi}}} \sqrt{2\rho\Delta p_{inj}} \tag{9}$$

Equation (9) may also be written as:

$$\dot{m}_{inj} = \mu_{inj} A_n \sqrt{2\rho\Delta p_{inj}} \tag{10}$$

where the A_n is the atomizer nozzle area. The discharge coefficient, μ_{inj}, is defined, for the inviscid flow in a swirl injector, as:

$$\mu_{inj} = \frac{1}{\sqrt{\frac{1}{\varphi^2} + \frac{K^2}{1-\varphi}}} \tag{11}$$

G. N. Abramovich (1946) noted that it is clear from Equation (11) that the discharge coefficient as a function of φ has small values for both small and large values of φ, passing through a maximum. As a result, a maximum value of K is observed, indicating the existence of the maximum flow rate for a given K. In accordance with the Principle of Maximum Flow (Abramovich, G. N.,1944), one may find that

$$K = \frac{(1-\varphi)\sqrt{2}}{\varphi\sqrt{\varphi}} \tag{12}$$

Hence, from Equation (11) the maximum discharge coefficient is

$$\mu_{inj} = \frac{\varphi\sqrt{\varphi}}{\sqrt{2-\varphi}} \tag{13}$$

and the average inviscid spray angle, $\overline{\alpha}$, can be written as:

$$\overline{\alpha} = \arctan\left\{\frac{(1-\varphi)\sqrt{8}}{\left[\left(1+\sqrt{1-\varphi}\right)\sqrt{\varphi}\right]}\right\} \tag{14}$$

Equations (13) and (14) reveal that, under the assumptions made, the discharge coefficient and spray cone angle are simply determined by the geometric characteristics and does not depend on the operating conditions of the atomizer.

Fluid viscosity and friction losses may be incorporated in Eqs. (11) and (14) by adding a momentum loss coefficient, ψ, and a resistance coefficient, ξ_{inj}, as follows:

$$\mu_{inj} = \frac{1}{\sqrt{\frac{2-\varphi}{\varphi^3} + \xi_{inj}\frac{K^2}{C^2}}} \tag{15}$$

and

$$\overline{\alpha} = \arcsin\left[\frac{2\mu_{inj}\left(\psi K\right)}{\left(1+\sqrt{1-\varphi}\right)\sqrt{1-\xi_{inj}\mu_{inj}^2\frac{K^2}{C^2}}}\right] \tag{16}$$

For low-viscosity fluids, ψ is usually close to unit. The resistance coefficient is obtained from test data, or by use of tables available in the literature (Vasiliev et al., 1993).

3. NUMERICAL SOLUTION

The CFD tool employed was the OpenFOAM version 1.6. OpenFOAM is a *C++ library* used primarily to create executables, known as *applications*. The applications are divided into two categories: *solvers*, assigned to actually solve a specific problem in continuum mechanics, and *utilities*, designed to provide a wide range of functionalities regarding pre- and post-processing. Being an *open source code*, OpenFOAM allows the creation of new solvers and utilities at user's discretion, as long as some pre-requisite knowledge of the underlying method, physics and programming techniques are concerned.

3.1 Governing equations

The solutions presented in this paper implements the laminar *volume of fluid* (VOF) equations. In the VOF capturing interface method, one momentum equation and one continuity equation are solved. These equations are the same for both fases, the physical properties of one fluid being calculated as a weighted-average based on the volume fraction of the two fluids in one cell. The momentum equation can be written as:

$$\frac{\partial\left(\rho\vec{W}\right)}{\partial t} + \nabla\bullet\left(\rho\vec{W}\vec{W}\right) - \nabla\bullet\mu\nabla\vec{W} - \rho\vec{g} = -\nabla p - \vec{F}_s \tag{17}$$

where μ is the dynamic viscosity and $\vec{F}_s$ is the surface tension force. The continuity equation assumes the form

$$\nabla\bullet\vec{W} = 0 \tag{18}$$

The volume of fluid in a cell is computed as $F_{vol} = \gamma V_{cell}$, where V_{cell} is the volume of a computational cell and γ is the fluid fraction in a cell. The values of γ range from 0 to 1. Therefore, a cell completely filled with fluid is represented by $\gamma = 1$; on the other hand, the void phase indicates a γ value equal to 0. At the interface γ assumes any value between 0 and 1. The scalar function γ is computed from a separate transport equation given by

$$\frac{\partial\gamma}{\partial t} + \nabla\bullet\left(\gamma\vec{W}\right) = 0 \tag{19}$$

In OpenFOAM, the necessary compression of the surface is achieved by introducing an extra artificial compression term into Eq. (19) as follows:

$$\frac{\partial \gamma}{\partial t} + \nabla \bullet \left(\gamma \vec{W}\right) + \nabla \bullet \left[\gamma \left(1-\gamma\right) \vec{U}_r\right] = 0 \tag{20}$$

where U_r is a velocity field suitable to compress the interface. This artificial term is active only in the interface region due to the term $\gamma\left(1-\gamma\right)$.

Fluid properties at any point in the domain are calculated as the weighted-average of the volume of fluid of the two fluids as:

$$\rho = \gamma\rho_1 + \left(1-\gamma\right)\rho_2 \tag{21}$$

$$\mu = \gamma\mu_1 + \left(1-\gamma\right)\mu_2 \tag{22}$$

where the subscripts 1 and 2 indicate the phases involved (a liquid and a gas, for example).

The surface tension F_s is computed as:

$$\vec{F}_s = \sigma\kappa\left(x\right)\vec{n} \tag{23}$$

where $\vec{n}$ is a unit vector normal to the interface that can be calculated as

$$\vec{n} = \frac{\nabla\gamma}{\left|\nabla\gamma\right|} \tag{24}$$

and κ is the curvature of the interface given by

$$\kappa\left(x\right) = \nabla \bullet \vec{n} \tag{25}$$

Equations (25) through (33) are implemented in the interFoam solver, through a pressure-implicit split-operator (PISO) algorithm, present in the OpenFOAM applications directory.

3.2 Fluid domain and boundary conditions

The solution was obtained for both the fuel and oxidizer core elements. The initial condition is defined by filling the entire fluid domain with stationary liquid. The imposed boundary conditions were a total pressure of 5 [bar] at the inlet and a static pressure of 1 [bar] at the outlet, thus giving the nominal 4 [bar] pressure drop.

The discretization of the fluid domain is accomplished by a powerful, yet not flawless, OpenFOAM utility. This tool generates three-dimensional grids containing primarily hexahedra and split-hexahedra automatically from surface geometries in Stereolithography (STL) format. Combined with adaptive mesh refinement, the mesh generation process is made easier. The final LOX injector mesh consisting of approximately 2.5 million points, is shown Fig. (1).

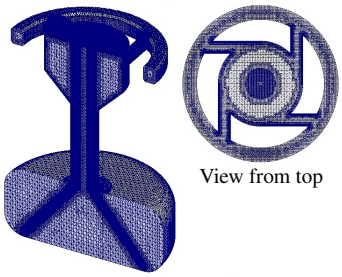

Figure 1. Final mesh obtained for the LOX atomizer.

3.3 Results

Using water to simulate the propellants and air as the gaseous phase, the cold flow solutions were pursued for both swirlers at the prescribed boundary conditions.

The velocity and thickness of the liquid film at the atomizer outlet, are of interest because they govern the breakup of the film. In both cases, especially in the LOX simulation, the interface between the liquid and gas phases become unsteady, displaying waves of small amplitude along its surface. The waves originate at the top of the atomizer, on the stagnation point on the wall, and propagate toward the exit, see Fig. 2b. The stagnation point leads to the formation of a crest at the fuel injector head end, as shown in Fig. 2a. The resulting flows are of highly three-dimensional character, where the air core is rotating, generating a spiraling disturbance on its surface. The Particle Image Velocimetry (PIV) technique was employed to evaluate the spray flow field; a summary of the results are presented in Fig. 3 for both atomizers.

Velocity components obtained in the simulations are depicted in Fig. 4 and Fig. 5. The axial component of velocity across an atomizer cross-section remained approximately constant, increasing along the length of the injector. From the CFD results we observe that the tangential velocity obeys a $1/r$ velocity profile and that the radial component is very small in comparison to axial and tangential components.

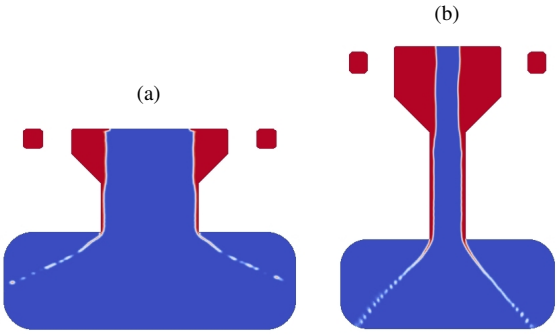

Figure 2. Phase fraction for the fuel (a) and oxidizer (b) atomizers.

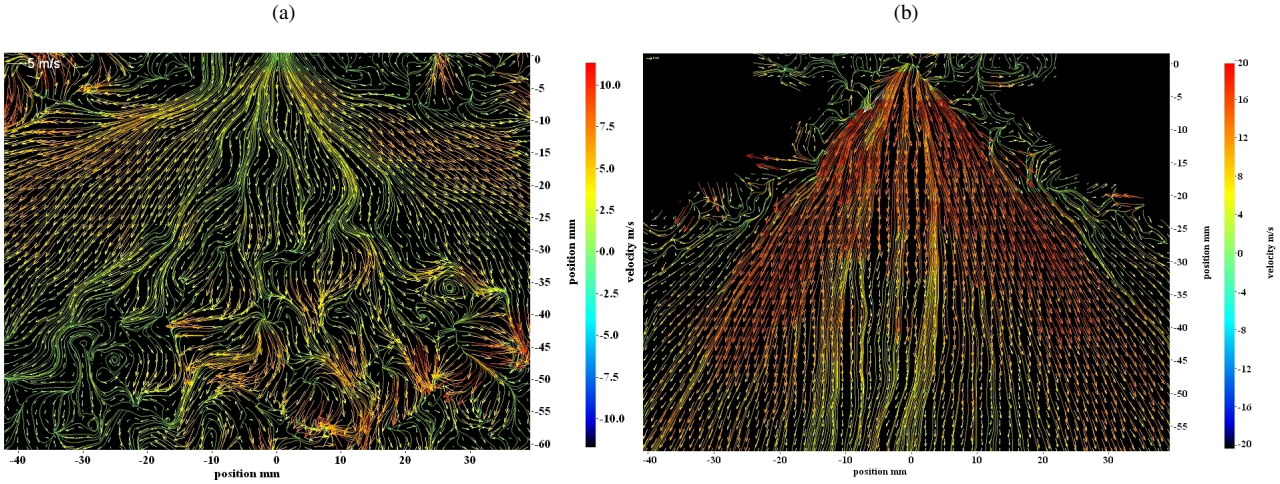

Figure 3. Fuel (a) and LOX (b) atomizers spray velocity field.

The main objective of this research is to evaluate CFD as a rocket injector analysis tool. The numerical simulation used a simple, laminar turbulence model. Comparing the initial CFD results to analytical and experimental results it became evident that the model did not represent perfect estimates of injector performance parameters, especially the discharge coefficient. The simulation then progressed with an iterative approach; that is modeling different fluid domains and improving mesh resolution by identifying weaknesses. However, after a series of simulations, it was clear that there were design and operational effects that were not accounted for in the CFD model. The data has been compiled in Tables 1 and 2 to compare theories in the literature and experimental test results to best evaluate the CFD analysis results.

The effects of friction are seen in both the measured cone angles and in the discharge coefficients. The cone angles came out in the range of 73 to 119 for the LOX swirler and 121 to 156 for the fuel swirler. The effect of viscosity is most keenly seen in the discharge coefficient, as the measured μ_{inj} is higher than that predicted by any of the inviscid models. This illustrates the paradoxical effect of swirl injectors that viscosity increases μ_{inj}. As the liquid swirls around the chamber and contracts, angular momentum is lost due to friction with the walls and is especially high in the tangential orifices where the velocities are the largest. This results in the film thickness being greater than predicted, and it is reasonable to assume that this contributes to inferior atomization.

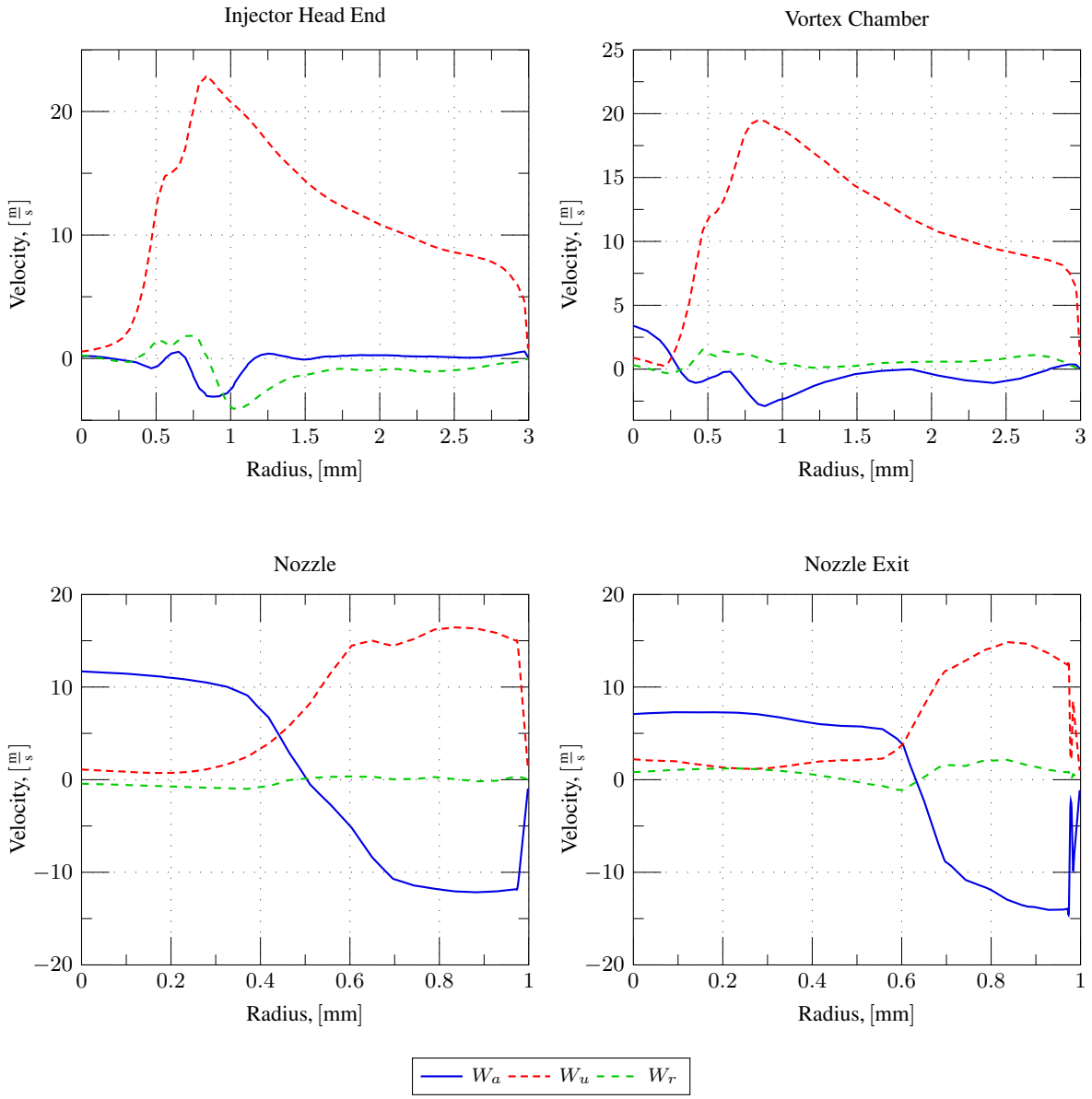

Figure 4. Velocity components along various LOX injector cross-sections.

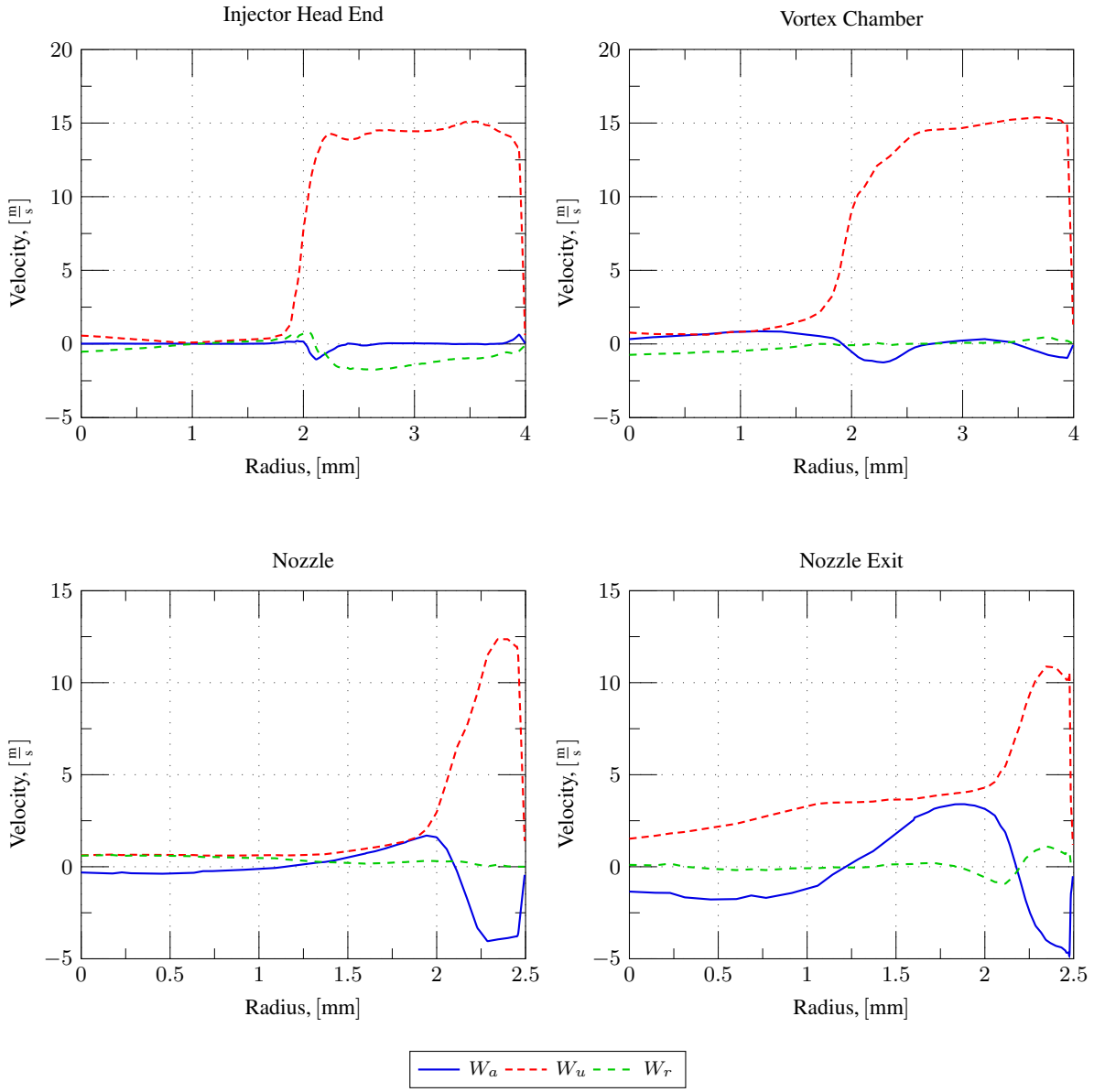

Figure 5. Velocity components along various fuel injector cross-sections.

Table 1. Summary of Analytical, Experimental and CFD Results for the LOX Swirler

	Parameter		
Model	$\dot{m}_{inj}$, [g/s]	μ_{inj}	$2\overline{\alpha}$, [degrees]
Abramovich [inviscid]	18,64	0,209	100
Abramovich [corrected]	19,44	0,219	94
Taylor	18,50	0,208	119
Bayvel and Orzechowski	18,13	0,204	108
Cold flow test	19,92±0,5	0,225±0,03	75±1,5
CFD	15,14±0,2	0,169±0,002	73

Table 2. Summary of Analytical, Experimental and CFD Results for the Fuel Swirler

	Parameter		
Model	$\dot{m}_{inj}$, [g/s]	μ_{inj}	$2\overline{\alpha}$, [degrees]
Abramovich [inviscid]	9,03	0,0163	155
Abramovich [corrected]	10,61	0,0191	121
Taylor	9,07	0,0163	156
Bayvel and Orzechowski	9,00	0,0162	150
Cold flow test	10,43±0,1	0,0188±0,002	128±1,5
CFD	8,82±0,03	0,0154±0,03	125

The laminar CFD simulation produced a similar value of spray angle in comparison with that obtained in the experiments. On the other hand, the water mass flow (or the discharge coefficient, μ_{inj}) was significantly lower for both atomizers. That discrepancy is presented in Table 3. Numerical and experimental values differ in 25 % and 18 % for the LOX and fuel swirlers, respectively; the corrected Abramovich model agrees well with the experiments, differing a maximum of 3 %. The inviscid Abramovich model is also included for the sake of completeness.

Table 3. Discrepancy in the Discharge Coefficient

Swirler	μ_{exp}	μ_{id}/μ_{exp}	μ_{corr}/μ_{exp}	μ_{num}/μ_{exp}
Inner (LOX)	0,23	0,93	0,97	0,75
Outer (JP-4)	0,019	0,87	1,02	0,82

4. CONCLUSION

The core injection element of a 5-[kN] was evaluated numerically using an Open Source CFD code and a laminar VOF turbulence model. This simplified model was able to match reasonably well the theoretical and experimental spray angle. Discrepancies of up to 25 %, however, were observed in the mass flow rate, in comparison to cold flow tests. Although significant, these deviations are well within those described in the available literature (Vasiliev et al., 1993). Despite that, more accurate predictions of atomizer spray cone angle and discharge coefficient. This can be accomplished by use of different turbulent models, such as LES or DNS. All in all, because of some simplifying assumptions used in the numerical simulation, the answers obtained from a laminar VOF model usually will not correspond exactly to those resulting from a careful analysis, but they should constitute a useful starting point in the trial and error procedure needed in a more detailed optimum injector design effort.

5. ACKNOWLEDGEMENTS

The authors would like to thank the Division of Space Propulsion for providing the preliminary experimental results.

6. REFERENCES

Abramovich, G. N., 1944, "The Theory of Swirl Atomizers", Industrial Aerodynamics, BNT ZAGI, Moscow, Russia.

Mikhailov, V. V. and Bazarov, V. G.,1985, "Throttlable Liquid Rocket Engines", Mashinostroyeniye Press, Moscow, Russia.

Chu, Chia-Chien and Chou, Shyan-Fu and Lin, Heng-I and Liann, Yi-Hai, 2008, "An experimental investigation of swirl atomizer sprays", Heat and Mass Transfer, Vol. 45, pp. 11-22.

Hinckel, J. N. and Villa Nova, H. F. and Bazarov, V. G., 2008, "CFD Analysis of Swirl Atomizers", 44th AIAA/ASME/SAE/ASEE Joint Propulsion Conference and Exhibit.

Giffen, E. and Muraszew, A., 1953, "Atomization of Liquid Fuels", Chapman and Hall, London.

Taylor, G., 1948, "The Mechanism of Swirl Atomizers", Proceedings of the 7th International Congress for Applied Mechanics, Vol. 2, London.

Kim, D. and Im, Ji-Hunk and Koh, H. and Yoon, Y., 2007, "Effect of Ambient Gas Density on Spray Characteristics of Swirling Liquid Sheets", Journal of Propulsion and Power, Vol. 23, No. 3, pp. 603-611.

Park, S. K. and Heister, S. D., 2010, "Nonlinear Modeling of Drop Size Distributions Produced by Pressure-Swirl Atomizers", International Journal of Multiphase Flow, Vol. 36, No. 1, pp. 1-12.

Vasiliev, A. P. and Kurpatenkov, V. M. and Kuznetsov, V. A. and Kurpatenkov, V. D. and Obelnitsky, A. M. and Poliaev, V. M. and Poliaev, B. I., 1993, "Ochnoviy Teori y racheta GRD" (in Russian), Moskwa Vischkaia Skola, Moscow, Russia.

7. Responsibility notice

The authors are the only responsible for the printed material included in this paper